Damage characterization in Dual-Phase steels using X-ray tomography

C. Landron [a], E. Maire [a], J. Adrien [a], O. Bouaziz [b]

[a] *INSA-Lyon, MATEIS UMR5510, 25 av. Capelle, 69621 Villeurbanne, France*
[b] *ArcelorMittal Research, Voie Romaine, 57283 Maizieres-les-Metz Cedex, France*

ABSTRACT

In-situ tensile tests have been carried out during X-ray microtomography imaging of dual-phase steels. Void nucleation has been quantified as a function of strain and triaxiality using the obtained 3D images. The Argon's criterion of decohesion has then been used in a model for nucleation in the case where martensite plays the role of inclusions. This criterion has been modified to include the local stress field and the effect of kinematic hardening present in such an heterogeneous material.

1 Introduction

Ductile damage is characterized by a three step process: cavities first nucleate, then grow, until coalescence leads to the ductile fracture. The first step of nucleation has been extensively studied and modeled. Void nucleation is usually associated to the presence of a second phase, like particles or inclusions. In the latter case, the cavities appear close to the inclusions, either inside the particle or at the interface [1-3]. Dual-Phase steels (DP steels) containing hard martensite islands embedded in a ductile ferritic matrix, are such kind of materials promoting inhomogeneous nucleation. In DP steels, the main nucleation mechanism is the interface decohesion as experimentally observed by [4, 5]. To model this interface debonding, an energy criterion [2,6,7] is necessary for the creation of new surfaces and a stress criterion [1,8] or a strain criterion [9,10] is required for breaking the bonds. To combine the two criteria, numerical models using cohesive zones have also been developed [11-13].
In order to be validated, these models have to be compared with key experiments. X-ray absorption microtomography is currently one of the most reliable ways to obtain quantitative three-dimensional (3D) information on damage [14,15]. In the present paper, damage in a DP steel is studied by in-situ tensile tests during X-ray microtomography imaging. Quantitative data is then used to validate an analytical modeling of void nucleation based on the Argon's criterion [1].

2 Experimental procedure

X-ray microtomography has been used in the present study to quantify damage during in-situ tensile tests. The method can be used for the imaging and the quantification of the microstructure of materials. Applications to study damage in ductile materials can be found in Refs. [14-16]. The tomography setup used is the one located at the ID15 beam line at the European Synchrotron Radiation Facility (ESRF) in Grenoble, France (more information is given in [17]). Tomography acquisition is carried out with a voxel size of $(1.6\mu m)^3$. With such a resolution, the smallest observed voids have a diameter of almost 2µm. Smaller voids, not accounted in the quantification, do exist in the sample but may not play a major role in damage.
The DP steel used for this study was cut from a 3 mm thick sheet obtained by hot rolling and thermal treatment. Its mechanical properties are given in Table 1. It has been checked by image analysis of optical micrographs of polished surfaces that the steel contains about 11% martensite. Axisymetric specimens were machined from the original sheet. Two kinds of specimen's shapes inspired by [18] were cut: two smooth samples and two samples with a 1 mm notch radius. The specimen's geometry is given in Fig.1. Each shape induces a different initial triaxiality. This allows us to study the effect of this important parameter on damage. Only the central part, 1.6 mm in height, is imaged during the present study.

Table 1 Mechanical properties in tension of the studied DP steel

Re (MPa)	Rm (MPa)	Ag (%)	A (%)
366	603	17.7	26.6

The fractured samples were polished after the in situ tensile test down to their central plane and etched with a 2 pct nital solution. The samples were dipped in a solution of ethanol and placed into a ultrasound cleaner for a duration of 30 minutes

T. Proulx (ed.), *Optical Measurements, Modeling, and Metrology, Volume 5*, Conference Proceedings of the Society for Experimental Mechanics Series 9999999, DOI 10.1007/978-1-4614-0228-2_2, © The Society for Experimental Mechanics, Inc. 2011

after the polishing to eliminate the possible fragments blunting the cavities. Light optical micrographs were then acquired in order to observe the nucleation sites.

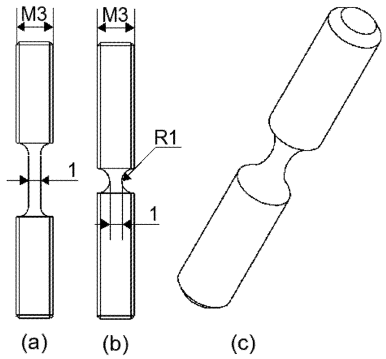

Fig.1 Tensile samples used: smooth specimen (a), 1mm radius notched specimen (b), 3D view (c)

3 Results and discussion

3-1 Damage characterization

X-ray microtomography imaging has already been used in order to visualize and quantify damage in DP steel in [17]. The same procedure was used in this study: raw processing were performed with the ImageJ freeware [19]. Initial volumes were median filtered and simply thresholded to differentiate material from voids. Damage can be qualitatively observed in 2D using sections inside the volume as ones presented in Fig.2 or in 3D using a global view of the sample as ones showed in Fig.3. 3D visualization softwares allow one to have a transparent view of some of the voxels (for instance those located in the solid phase) and then lead to the possibility of seeing cavities inside the sample. Tomography volumes can also be employed to quantify damage appearing during the tensile test. As in [17], only the central part of the tensile specimen is used for this damage quantification. This sub-region was chosen to be a cubic volume of $(300\mu m)^3$. Fig.4. shows this studied sub-region in a notched specimen of DP steel at several steps of deformation. This qualitative figure shows clearly that the number of cavities increases (nucleation) and that the size of the nucleated cavities also increases (growth) with the increase of strain. It is noticeable in this image that nucleation is a quantitatively important part of the damage progression in these materials, as evidenced already in [17]. Each pore of the volume is then subsequently labeled using a dedicated image processing plugin implemented in the ImageJ [19] freeware. The labeling plugin uses a binary image as input. It simply detects the 3D clusters of connected voxels and gives a label to each. The void density is calculated as the number of cavities per cubic millimeter in the sub-volume. The volume of each cavity is also measured as well as its dimensions permitting to quantitatively characterize the growth and the shape change of voids during the tensile deformation.

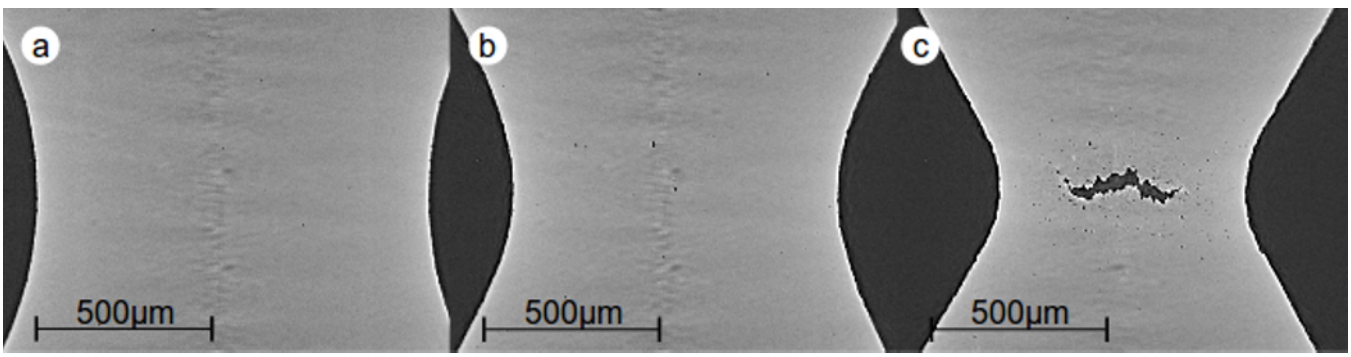

Fig.2 Sections at the center of a notched strained specimen at various steps of deformation: ε_{loc}=0 (a), ε_{loc}=0.35 (b) and ε_{loc}=0.83 (c)

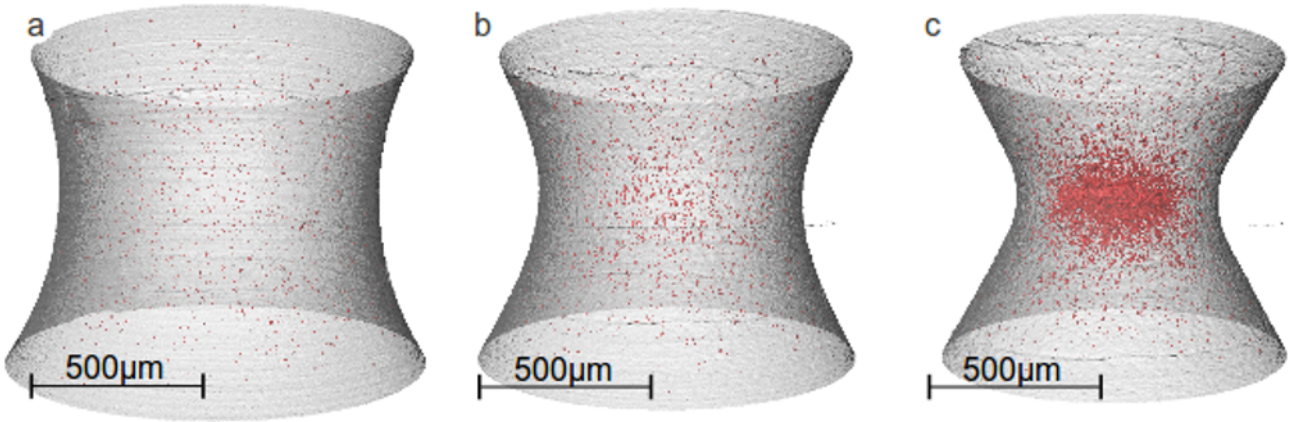

Fig.3 3-D views of a notched strained specimen at various steps of deformation: ε_{loc}=0 (a), ε_{loc}=0.35 (b) and ε_{loc}=0.83 (c). The outline of the specimen appears in gray and the cavities in red

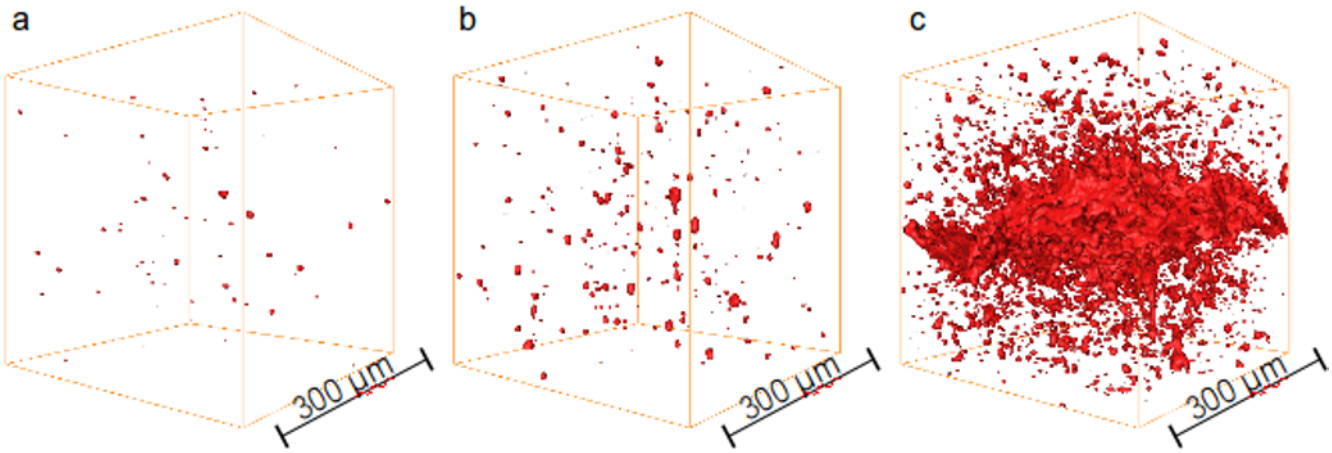

Fig.4 3-D views of damage at the center of a notched strained specimen at various steps of deformation: ε_{loc}=0 (a), ε_{loc}=0.35 (b) and ε_{loc}=0.83 (c)

Some mechanical parameters were calculated using the outside shape of the specimen. The minimal section area S was measured in order to calculate the local strain ε_{loc} at each step using equation (1):

$$\varepsilon_{loc} = \ln\left(\frac{S_0}{S}\right) \quad (1)$$

S_0 being the initial section of the sample. This equation implies that the effect of porosity in the volume change of the sample is neglected in our analysis.

The curvature radius R_{notch} is also measured in order to determine the stress triaxiality T using equation (2), derived from the Bridgman analysis of notched bars [20].

$$T = \frac{1}{3} + \ln\left(1 + \frac{a}{2R_{notch}}\right) \quad (2)$$

a being the radius of the minimal section, easily tractable from the value of S.

Fig.5. shows the evolution of N, the number of voids per unit volume (expressed per cubic mm) in several DP steel samples with smooth and notched geometries. A very small amount of porosity (0.03%) can be detected before the tensile test, may be due to the fabrication process. The experimental results show that the triaxiality has a straightforward impact on the nucleation kinetic: void nucleation occurs earlier in notched samples inducing higher triaxiality than in smooth samples.

Optical micrographs performed on the fractured specimens and given in Fig.6. show that most cavities are localized between the ferritic matrix and martensite islands and thus nucleate by decohesion of the ferrite/martensite interface as previously observed in [4, 5].

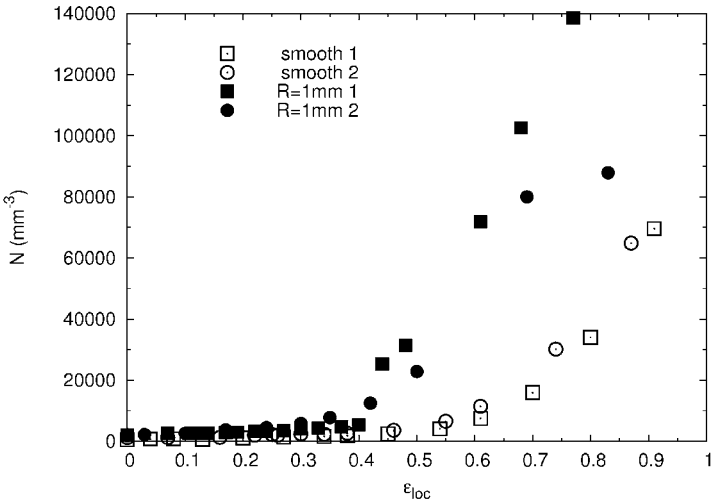

Fig.5 Evolution of *N*, the number of cavities per cubic mm in the four studied samples measured during the in-situ tensile tests [21]

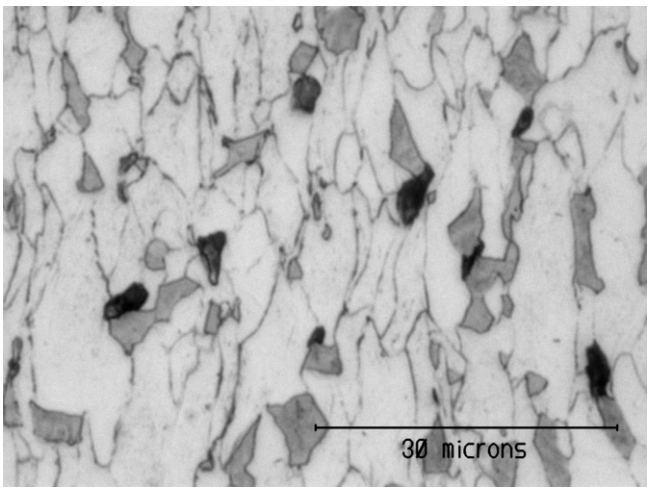

Fig.6 Micrograph of fractured specimen. Voids appear in black, ferrite in light gray and martensite in dark gray [21]

3-2 Void nucleation modeling

As demonstrated by [6], the energy criterion necessary for the creation of new surfaces at the inclusion/matrix interface is satisfied at the onset of plastic deformation in materials containing inclusions bigger than about 25 nm in diameter. Only a stress criterion will therefore be used to model the interface decohesion in DP steels as the observed inclusions are about 100 times larger than this. The Argon's criterion [1] is a critical stress criterion stating that the void nucleation occurs when a critical stress state, necessary for the interface decohesion, is reached in the material. This stress state involves a contribution of the hydrostatic stress σ_m and the equivalent stress σ_{eq}.

$$\sigma_{eq} + \sigma_m = \sigma_C \quad (3)$$

where σ_C is the interface strength, e.g. the maximum shear stress that the interface can support without breaking.

The interest in using the Argon's criterion lies in the fact that it accounts for the triaxiality T (T being the ratio between σ_{eq} and σ_m).

$$T = \frac{\sigma_{eq}}{\sigma_m} \quad (4)$$

Combining Eq. (3) and Eq. (4), the criterion can be expressed as:

$$\sigma_{eq}(1 + T) = \sigma_C \quad (5)$$

In the original Argon's criterion, the triaxiality used is the macroscopic triaxiality. However, decohesion is a local

phenomenon which occurs at the interface of ferrite and martensite islands. In [22], it is demonstrated that the local triaxiality is higher at the interface because of the kinematic hardening X generated by the difference in mechanical behaviors of both phases. In DP steels, the difference between the mechanical behavior of the ferrite and martensite is quite high. Therefore it would be better to use the local triaxiality at the interface T_{loc}. T_{loc} can be estimated using the following expression coming from [22]:

$$T_{loc} = T\left(\frac{\sigma_{eq}}{\sigma_{eq} - X}\right) \qquad (6)$$

The modified expression of the Argon's criterion to get a local decohesion then becomes:

$$\sigma_{eq}\left(1 + T\left(\frac{\sigma_{eq}}{\sigma_{eq} - X}\right)\right) = \sigma_C \qquad (7)$$

The left side of the equation of this local version of the Argon's criterion is hereafter named χ.

By calculating the value of χ at the nucleation strain ε_N, an average value of σ_C can be estimated in the case of ferrite/martensite interface. ε_N is determined from the quantitative data obtained from the cavity measurements of the smooth samples. Its value is taken at the point when the void density starts to increase. Values of 0.18 and 0.02 are respectively found for the smooth samples and the notched samples. σ_{eq} is taken from the experimental true stress tensile curve and T is calculated with the Bridgman formula [20]. The value of the kinematic part of the hardening X is estimated from the formula given by [24] and modified to be expressed as a function of the respective hardness of ferrite HV_f and martensite HV_m:

$$X = 3\,(1 - f_m)\,f_m\,|HV_m - HV_f| \qquad (8)$$

where f_m is the volume fraction of martensite. Assuming that all the carbon present in the studied DP steel is located in the martensitic phase, the carbon content of the martensite is 0.73 wt.%. Regarding the work done by Grange on the prediction of martensite hardness [24], the value of HV_m is about 830 MPa. The hardness of the ferritic phase is taken as 150 MPa. The evolution of χ in the smooth and in the notched specimen with the deformation is given in Fig.7. The value of the interface's strength found here for this particular value of strain when nucleation starts to increase is equal to about 1100 MPa. A compilation of values for the strength of the interface between other particles and ferrite found by different authors is listed in Table 2. The order of magnitude is the same as the one calculated using our approach, the case of ferrite/martensite being situated in the lower range of these values. Note that our estimation is valid for the very beginning of the nucleation (i.e. when the number of voids starts to increase as seen in the tomography images). The other values being obtained with other methods and probably with other definitions, a direct comparison is not the aim of the presented table.

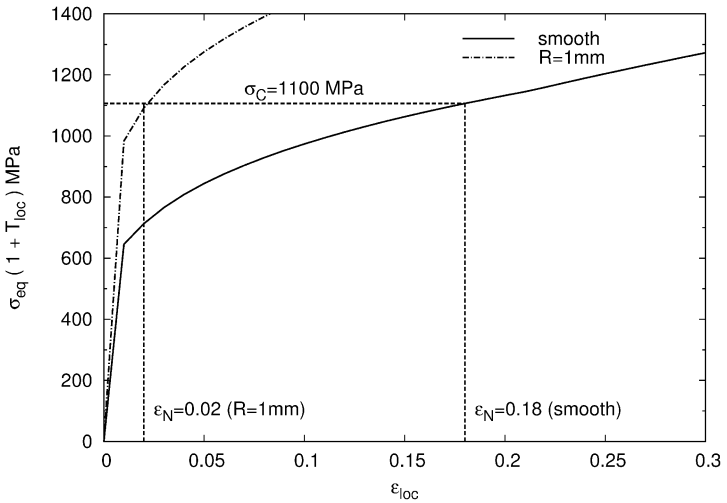

Fig.7 Calculation of the ferrite/martensite interface using χ

Table 2 Value of ferrite particle interface strength

Particle	Interface strength (MPa)	Ref.
Y_2O_3	1000-1600	[25]
MnS	1100-1400	[26]
Fe_3C	1200-2000	[27,28]

As pointed out in [5], void nucleation in DP steels occurs during the entire deformation process, i.e. each different single interface probably exhibits a different value of ε_N and each interface is possibly subjected to a scattered value of χ. Interface decohesion is thus a progressive phenomenon, starting for a strain of 0.18 (in smooth specimens) but continuing after this value of strain and the evolution of the cavity density has to be modeled as a function of the local strain. Fig.5 shows that the studied material exhibits two different nucleation regimes at low and at high strain. Firstly, the number of cavities increases slowly and linearly. In a second regime many voids appear exponentially. This experimental observation leads us to propose the following empirical equation based on the local criterion of decohesion and involving the parameters χ and σ_C.

$$\frac{dN}{d\varepsilon_{loc}} = A\frac{\chi}{\sigma_C}\left(1+\frac{N}{N_0}\right) \quad (9)$$

A and N_0 being two constants (expressed in the same unit as N, for instance in mm^{-3}).

The two extreme regimes are well described by this empirical expression. When $N \ll N_0$ the following approximation can be done:

$$\frac{dN}{d\varepsilon_{loc}} \approx A\frac{\chi}{\sigma_C} \quad (10)$$

The interface decohesion is then only linearly controlled by the local stress χ which increases with the applied strain. In the second regime, when $N \gg N_0$ the approximation becomes :

$$\frac{dN}{d\varepsilon_{loc}} \approx A\frac{\chi}{\sigma_C}\frac{N}{N_0} \quad (11)$$

The evolution rate of N with strain is proposed to depend on N itself, transcribing a self catalytic effect and thus the exponential acceleration of the number of cavities.

We then now have a mean to integrate the value of N, by accounting for the local triaxiality at the interface. The assessment of the model is firstly done using experimental data from smooth specimens. The values of the two constants A and N_0 giving the best fit between modeling and experimental data for the smooth sample are A=4500mm^{-3} and N_0=1250mm^{-3}. These values, when used in the framework of the notched samples, also show a satisfactory agreement as shown in Fig.8. This validates that using a local value of the triaxiality as a driving force in an interface fracture criterion is a reasonable procedure.

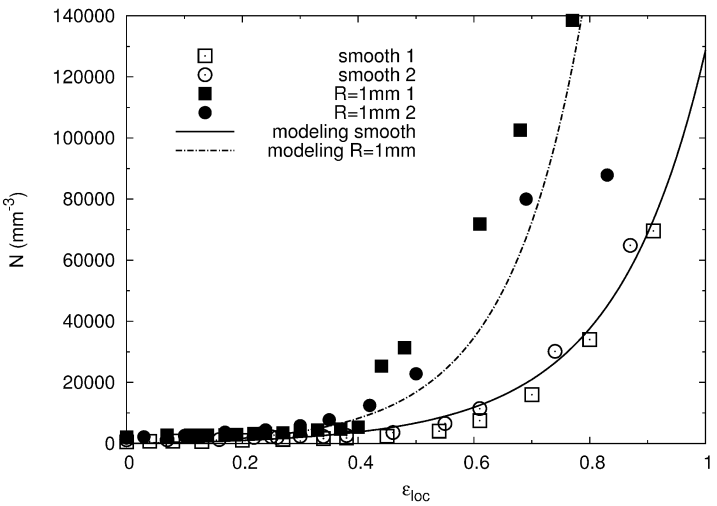

Fig.8 Comparison of the prediction of the nucleation model and experimental data [21]. The constants of the model are fitted to reproduce the experimental evolution in the case of the smooth sample and are then used "as-is" to calculate the evolution of the notched sample.

4 Conclusions and perspective

Using in-situ tensile tests during X-ray tomography, the present study has shown that it is possible to obtain quantitative information about damage. Concerning the sites of nucleation, optical micrographs of fractured samples have shown that most cavities appear by decohesion of the ferrite/martensite interface. A value of the critical interface strength (1100 MPa)

has been estimated for the onset of nucleation. The evolution of the void density has then been modeled according to an analytical approach based on a local version of the Argon decohesion criterion and accounting for the triaxiality. The model has been fitted with the experimental data on the smooth samples. The identified parameters were then used for the notched sample and also lead to a satisfactory agreement of the predicted evolution of the number of nucleated cavities. Some improvements could be foreseen in the present approach, particularly concerning the value of the interface strength in DP steels. This strength probably depends on the carbon content in the martensite and on an eventual tempering. These effects have to be investigated in more details before being modeled.

Acknowledgments

The authors would like to thank the ESRF for the provision of synchrotron radiation at the ID15 beamline through the ma560 long term project.

References

[1] Argon AS, Im J, Safoglu R, Cavity formation from inclusions in ductile fracture, Metallurgical Transactions A, Volume 6, Issue 4, pp 825-837, 1975.
[2] Goods SH, Brown LM, Nucleation of cavities by plastic-deformation – Overview, Acta Metallurgica,Volume 27, Issue 1, pp 1-15,1979.
[3] Beremin FM,Cavity formation from inclusions in ductile fracture of A508 steel, Metallurgical and Materials Transactions A, Volume 12, Issue 5, pp 723-731,1981.
[4] Steinbrunner DL, Matlock DK, Krauss G, Void formation during tensile testing of dual phase steels, Metallurgical Transactions A, Volume 19, Issue 3, pp 579-589,1988.
[5] Avramovic-Cingara G, Saleh CAR, Jain M, Wilkinson DS, Void Nucleation and Growth in Dual-Phase Steel 600 during Uniaxial Tensile Testing, Metallurgical and Materials Transactions A, Vlume 40, pp 3117-3127, 2009.
[6] Tanaka K, Mori T, Nakamura T, Cavity formation at the interface of a spherical inclusion in a plastically deformed matrix, Philosophical Magazine, Volume 21, Issue 170, pp. 267–279, 1970.
[7] Thomason PF, Ductile Fracture of Metals, Pergamon Press, Oxford, 1990.
[8] Kwon D, Asaro RJ, A study of void nucleation, growth, and coalescence in spheroidized-1518 steel, Metallurgical Transactions, Volume 21, Issue 1, pp 91-101, 1990.
[9] Walsh JA, Jata KV, Starke EA, The influence of Mn dispersoid content and stress state on ductile fracture of 2134 type Al-alloys, Acta Metallurgica, Volume 37, Issue 11, pp 2861-2871, 1989.
[10] Bugat S, Besson J, PineauA, Micromechanical modeling of the behavior of duplex stainless steels, Computational Materials Science, Volume 16, Issue 1-4, 158-166, 1999.
[11] Needleman A, A continuum model for void nucleation by inclusion debonding, Journal of Applied Mechanics, Volume 54, pp 525-531, 1987.
[12] Needleman A, Tvergaard V, An analysis of ductile rupture in notched bars, Journal of the Mechanics and Physics of Solids, Volume 32, Issue 6, pp 461-490, 1984.
[13] Nutt SR, Needleman A, Void nucleation at fiber ends in Al-SiC composites, Scripta Materialia, Volume 21, Issue 5, pp 705-710, 1987.
[14] Buffiere JY, Maire E, Cloetens P, Lormand G, Fougères R, Characterization of internal damage in a MMCp using x-ray synchrotron phase contrast microtomography, Acta Materialia, Volume 47, Issue 5, pp 1613-1625, 1999.
[15] Martin CF, Josserond C, Salvo L, Blandin JJ, Cloetens P, Boller E, Characterisation by X-ray micro-tomography of cavity coalescence during superplastic deformation, Scripta Materialia, Volume 42, Issue 4, pp 375-381, 2004.
[16] Babout L, Maire E, Fougeres R, Damage initiation in model metallic materials: X-ray tomography and modelling, Acta Materialia, Volume 52, Issue 8, pp 2475-2487, 2004.
[17] Maire E, Bouaziz O, Di Michiel M, Verdu C, Initiation and growth of damage in a dual-phase steel observed by X-ray microtomography, Acta Materialia, Volume 56, Issue 18, pp 4954-4964, 2008.
[18] Bron F, Besson J, Pineau A, Ductile rupture in thin sheets of two grades of 2024 aluminum alloy, Materials Science and Engineering A, Volume 380, Issue 1-2, pp 356-364, 2004.
[19] Abramoff MD, Magelhaes PJ, Ram SJ, Image Processing with ImageJ, Biophotonics International, Volume 11, Issue 7, pp 36-42, 2004.
[20] Bridgman PW, Effects of High Hydrostatic Pressure on the Plastic Properties of Metals, Revue of Modern Physics, Volume 17, Issue 1, pp 3-14, 1945.
[21] Landron C, Bouaziz O, Maire E, Characterization and modeling of void nucleation by interface decohesion in dual phase steel, Scripta Materialia, Volume 63, Issue 10, pp 973-976, 2010.
[22] Helbert AL, Feaugas X, Clavel M, Effects of microstructural parameters and back stress on damage mechanisms in

alpha/beta titanium alloys, Acta Metallurgica, Volume 46, Issue 3, 939-951, 1998.
[23] Allain S., Bouaziz O., Microstructure based modeling for the mechanical behavior of ferrite-pearlite steels suitable to capture isotropic and kinematic hardening, Materials Science and Engineering A, Volume496, Issue 1-2, pp 329-336, 2008.
[24] Grange RA, Hribal CR, Porter LF, Hardness of tempered martensite in carbon and low-alloy steels, Metallurgical Transactions A, Volume 8, Issue 11, pp 1775-1787, 1977.
[25] Kosco JB, Koss DA, Ductile fracture of mechanically alloyed iron-yttria alloys Metallurgical Transactions A, Volume 24, Issue 3, pp 681-687, 1993.
[26] Qiu H, Mori H, Enoki M, Kishi T, Development of A Three-dimensional Model for Void Coalescence in Materials Containing Two Types of Microvoids,ISIJ International, Volume 39, Issue 4, pp 358-364, 1999.
[27] LeRoy G, Embury JD, Edwards G, Ashby MF, A model of ductile fracture based on the nucleation and growth of voids, Acta Metallurgica, Volume 29, Issue 8, pp 1509-1522, 1981.
[28] Kwon D, Interfacial decohesion around spheroidal carbide particles, Scripta Metallurgica, Volume 22, Issue 7, pp 1161-1164, 1988.

http://www.springer.com/978-1-4614-0227-5

Optical Measurements, Modeling, and Metrology, Volume 5
Proceedings of the 2011 Annual Conference on Experimental and Applied Mechanics
Proulx, T. (Ed.)
2011, X, 422 p., Hardcover
ISBN: 978-1-4614-0227-5